Dynamic Regulation of Intact and C-Terminal Truncated Insulin Receptor Phosphorylation in Permeabilized Cells†

Michel Bernier,*,‡ Anthony S. Liotta,‡ Hemanta K. Kole,‡ David D. Shock,‡ and Jesse Roth§

Diabetes Unit, Laboratory of Clinical Physiology, National Institute on Aging, National Institutes of Health, Baltimore, Maryland 21224, and Department of Medicine, Division of Geriatric Medicine and Gerontology, The Johns Hopkins University School of Medicine, Baltimore, Maryland 21224

Received October 14, 1993; Revised Manuscript Received January 4, 1994®

ABSTRACT: Using digitonin-permeabilized Chinese hamster ovary (CHO) cells that were transfected with intact human insulin receptors (CHO/HIRc cells), we examined insulin receptor phosphorylation and dephosphorylation using pulse–chase techniques. Insulin activated receptor autophosphorylation on tyrosyl residues to a level severalfold over basal, reaching maximal levels after 2, 5, and 10 min of stimulation at 34, 18, and 6 °C, respectively. Phosphopeptide analysis revealed that the triply phosphorylated form of the 1146-kinase domain of the insulin receptor was the major species, which is characteristic of the fully active tyrosine kinase function. The dephosphorylation reaction was time- and temperature-dependent with $t_{1/2}$ values of 0.67 and 2 min at 18 and 6 °C, respectively. Vanadate completely inhibited dephosphorylation. Under similar permeabilization conditions when compared with CHO/HIRc cells, CHO/ΔCT cells (CHO cells overexpressing a mutated form of the receptor with a 43 amino acid deletion at the C-terminus) stimulated with insulin exhibited larger increases in receptor autophosphorylation levels and in tyrosine kinase activity toward a synthetic peptide substrate; the rate of CHO/ΔCT receptor dephosphorylation was not reduced. There was near-complete absence of insulin receptor substrate 1 (IRS-1) in the cell ghosts after permeabilization. We therefore examined the pattern of tyrosine phosphorylation and dephosphorylation of residual cellular proteins in permeabilized CHO/HIRc cells by Western blot analysis. In addition to the 95-kDa receptor β-subunit, we detected the phosphorylation of two glycoproteins which included the commonly found 120-kDa protein and a novel 195-kDa protein whose dephosphorylation rate is slower than that of receptor β-subunit. We conclude that there is an intimate association between insulin receptor and the protein(s) involved in the dephosphorylation cascade which is maintained in these permeabilized cells, even in the absence of IRS-1. This cell system allows new insights into insulin action (independent of IRS-1) by studying the effect of biological substances on the dynamic regulation of receptor phosphorylation and dephosphorylation as well as tyrosine kinase activity of the receptor β-subunit.

For insulin to produce its biological effects *in vivo*, insulin in the extracellular fluid binds to the extracellular domain of the insulin receptor; the receptor spans the plasma membrane and thereby links the outside and inside of the cell. The binding of the hormone stimulates the receptors's ability to phosphorylate specific tyrosyl residues within the intracellular (cytoplasmic) domain of the insulin receptor. This self-phosphorylation reaction activates the receptor's intrinsic tyrosine kinase activity toward other substrates and thereby triggers a cascade of events that ultimately leads to the metabolic and mitogenic effects associated with insulin [for a review, see Rosen (1987) and Kahn et al. (1993)].

The active form of the insulin receptor has a short half-life, because cellular phosphatase(s) remove(s) the phosphate moieties from the receptor molecule, deactivating it and thereby terminating insulin's action (Rosen et al., 1983; Häring et al., 1984; King & Sale, 1990). To date, the physiologically important protein tyrosine phosphatase(s) (PTPases)[1] that inactivate the insulin receptor remain unidentified; PTPase activities present in various tissue extracts and individual recombinant PTPases with markedly divergent structures dephosphorylate many peptide substrates, the insulin receptor, and other intact tyrosine phosphorylated receptors (King & Sale, 1988; Roome et al., 1988; Meyerovitch et al., 1989; Tappia et al., 1991; Boylan et al., 1992; Hashimoto et al., 1992; Ramachandran et al., 1992). This suggests that the specificity of the receptor-inactivating dephosphorylation process *in vivo* may depend less on the specificity of the enzyme–substrate interaction and be largely based on other mechanisms for establishing a high degree of specificity, e.g., intimate physical links generated by cell compartmentalization, substrate activation of phosphatase, specific recognition sites distinct from the enzyme–substrate domain, and links effected by intermediate molecules.

In this study, we investigated whether a dynamic regulation operates between insulin receptor phosphorylation and dephosphorylation in cells overexpressing human insulin receptors; these transfected cells have been used extensively to study various aspects of the insulin signaling pathway. These include stimulation of receptor autophosphorylation and tyrosine

† These studies were presented, in part, at the June 1993 meeting of the Endocrine Society in Las Vegas, NV.

* To whom correspondence should be addressed at the Diabetes Unit, Gerontology Research Center, Room 2B-01, National Institute on Aging, 4940 Eastern Ave., Baltimore, MD 21224. Telephone: (410) 558–8198. Fax: (410) 558–8381.

‡ National Institutes of Health.

§ The Johns Hopkins University School of Medicine.

® Abstract published in *Advance ACS Abstracts*, March 15, 1994.

[1] Abbreviations: CHO, Chinese hamster ovary; CHO/HIRc, CHO cells overexpressing the normal human insulin receptor; CHO/ΔCT, CHO cells overexpressing a mutant form of the receptor which lacks the 43 amino acids at the C-terminus of the β-subunit; PTPase, protein tyrosine phosphatase; IRS-1, insulin receptor substrate 1; PVDF, poly(vinylidene difluoride); SDS–PAGE, SDS–polyacrylamide gel electrophoresis; WGA, wheat germ agglutinin; EDTA, ethylenediaminetetraacetic acid; TBS-T, tris(hydroxymethyl)aminomethane-buffered saline containing 0.1% Triton X-100.

0006-2960/94/0433-4343$04.50/0

kinase activity toward endogenous and exogenous substrates (Ellis et al., 1986; Chou et al., 1987; White et al., 1987), glycogen synthesis (McClain et al., 1987; Debant et al., 1988), phosphatidylinositol 3-kinase activation (Endemann et al., 1990; Ruderman et al., 1990), and mitogenic activity (Chou et al., 1987; Ebina et al., 1987; Maegawa et al., 1988). While important information has been gained from these studies, little is known about the dynamic regulation of tyrosine phosphorylation and dephosphorylation of the overexpressed insulin receptor. We examined the kinetics of these processes in digitonin-permeabilized cultured Chinese hamster ovary (CHO) cells transfected with the cDNA encoding the normal human insulin receptor (CHO/HIRc). To clarify whether the C-terminal domain of the insulin receptor plays an anchoring function for PTPase(s), we also examined a CHO cell line expressing a mutant form of the receptor which lacks 43 amino acids at the C-terminus of the β-subunit (CHO/ΔCT). We used a procedure similar to that used to study insulin receptors in adipocytes (Mooney & Anderson, 1989) based on cell permeabilization by the steroid glycoside digitonin, which gives small molecules (e.g., [γ-^{32}P]ATP, cations, EDTA) free access to the intracellular domain. This allowed us (1) to monitor the rapid kinetics of receptor phosphorylation and dephosphorylation to a degree that has been impossible with intact cells and yet retain much of the membrane architecture of the *in vivo* system, (2) to show that the truncated receptor has an enhanced tyrosine kinase activity without inhibition of receptor dephosphorylation, and (3) to demonstrate that insulin receptor substrate 1 is not required for activation or deactivation of the insulin receptor.

EXPERIMENTAL PROCEDURES

Materials. All chemicals used were analytical grade. Tissue culture media were purchased from NIH media service and Quality Biologicals (Gaithersburg, MD), sera from Hyclone (Logan, UT), digitonin from Calbiochem (La Jolla, CA), bovine serum albumin (fraction V) from Intergen (Purchase, NY), agarose-bound wheat germ agglutinin and protein A–agarose beads from Vector Laboratory (Burlingame, CA), and *N*-acetylglucosamine and 2-mercaptoethanol from Sigma (St. Louis, MO). Cellulose plates were purchased from Kodak (Rochester, NY). Electrophoresis supplies were from BioRad (Hercules, CA). Precasted gradient SDS–PAGE gels and poly(vinylidene difluoride) (PVDF) membranes were from Novex (San Diego, CA). Recombinant human insulin, anti-phosphotyrosine polyclonal antibody, anti-human IRS-1 polyclonal, and monoclonal antibodies were purchased from Upstate Biotechnology Inc. (Lake Placid, NY). The anti-insulin receptor monoclonal antibody, 29B4, and protein G-Plus/protein A–agarose were from Oncogene Science (Manhasset, NY). The anti-insulin receptor β-subunit polyclonal antibody, AB-50, was a gift from Dr. Domenico Accili (National Institutes of Health, Bethesda, MD). [γ-^{32}P]-ATP (~3000 Ci/mmol), Rainbow protein molecular weight markers, donkey anti-rabbit IgG–horseradish peroxidase conjugate, and Enhanced Chemoluminescent (ECL) detection system were from Amersham (Arlington Heights, IL). Goat anti-mouse IgG–horseradish peroxidase conjugate was from Pierce (Rockford, IL). A synthetic peptide corresponding to residues 983–993 of the insulin receptor substrate 1 (peptide 983–993: Ser-Arg-Gly-Asp-Tyr-Met-Thr-Met-Gln-Ile-Gly) was synthesized in our laboratory using HOBt/NMP-FMOC chemistry on an Applied Biosystems 430A automatic solid-phase peptide synthesizer and purified by reversed-phase HPLC; its structure was confirmed by mass spectroscopy (kindly performed by Dr. H. N. Fales, NIH).

Cell Lines. The two Chinese hamster ovary (CHO) cell lines (generous gift from Dr. Morris F. White, Joslin Diabetes Center, Boston, MA) used in this study have been previously described (Chou et al., 1987; Myers et al., 1991). These include the CHO cell line transfected with an expression plasmid encoding the normal human insulin receptor (CHO/HIRc) and the CHO cell line expressing a mutant form of the receptor which lacks the 43 amino acids at the C-terminus of the β-subunit (CHO/ΔCT). The cells were maintained in F-12 medium containing 10% fetal bovine serum and were cultured to confluence.

Permeabilization of Cells and Autophosphorylation and Dephosphorylation of Insulin Receptors. Confluent monolayers of CHO cells lines in 3.5-cm dishes (Falcon) were incubated in serum-free F-12 medium for 3–5 h at 37 °C and then washed with phosphate-buffered saline at pH 7.4. The medium was replaced with permeabilization medium A that contained, at final concentrations, 35 μg/mL digitonin, 20 mM Tris (pH 7.5), 125 mM potassium chloride, 5 mM sodium chloride, 10 mM magnesium chloride, 11.1 mM glucose, and 0.1% (w/v) albumin. After 20 min at room temperature, the culture dishes with the cells still in permeabilization medium were transferred to an aluminum cooling plate (Pharmacia) connected to a thermostatic water circulator (Lauda). Selected circulator settings maintained the temperature in dishes at 6, 18, and 34 °C; readings were obtained using a digital thermocouple thermometer (Ebro) mounted with a microprobe. After 2 min on the plate at the selected temperature, the cells were incubated with 100 nM insulin for 15 min, and then the phosphorylation reaction was initiated by adding labeling medium containing at final concentrations 100 μM [γ-^{32}P]ATP (1.7 μCi/nmol) and 4 mM manganese chloride. At the indicated times, the cells were rapidly frozen with liquid nitrogen.

After the [γ-^{32}P]ATP phosphorylation reaction had reached an apparent steady-state (between 5 and 10 min, depending on the temperature of incubation), the phosphorylation was halted to permit monitoring of the dephosphorylation of the insulin receptor. To accomplish this, we added a 20-μL aliquot of a chase solution containing at final concentrations 20 mM EDTA (to chelate divalent cations) and 4 mM unlabeled ATP. The residual phosphorylation state of the receptor was monitored at various time intervals thereafter. Dithiothreitol has been reported to be essential for effective receptor dephosphorylation in *in vitro* membrane-based assays (Lau et al., 1989; Tonks et al., 1989; Faure et al., 1992), possibly because the essential cysteinyl residue in the PTPase catalytic domain (Streuli et al., 1990; Guan & Dixon, 1991) is oxidized during membrane preparation, requiring reduction to reconstitute PTPase activity. A sulfhydryl reagent was not required for the dephosphorylation reaction to proceed in the permeabilized cells.

The cells were solubilized as described previously (Bernier et al., 1988) with slight modifications. In brief, cells were scraped into solubilization buffer [25 mM Tris (pH 7.6) containing 192 mM glycine, 25 mM EDTA, 25 mM EGTA, 100 mM sodium fluoride, 30 mM sodium pyrophosphate, 10 mM β-glycerophosphate, 1 mM sodium vanadate, 1 mM *N*-ethylmaleimide, 0.2 mM phenylmethanesulfonyl fluoride, 8 μg/mL aprotinin, 2 μg/mL leupeptin, 1.5% Triton X-100, and 0.06% SDS] and the cell extracts incubated for 60 min on ice. After removal of cell debris by centrifugation (14000*g*, 20 min), the supernatant was gently mixed with wheat germ

agglutinin–agarose to bind the insulin receptors. After 16 h at 4 °C, the resin was washed 3 times with buffer containing 0.1% Triton X-100 followed by elution of the bound glycoproteins by addition of 1.5 × concentrated Laemmli sample buffer containing 0.45 M *N*-acetylglucosamine. The eluted proteins were subjected to SDS–PAGE under reducing conditions (Laemmli, 1970) on Hoeffer Mighty Small dual-slab cells using 4.5% stacking and 7.5% separating polyacrylamide gels. The ^{32}P-labeled insulin receptor β-subunit was identified by autoradiography of the dried gels at −70 °C using enhancing screens and Amersham Hyperfilm-MP films, and quantified with a Betascope 603 blot analyzer (Betagen; Waltham, MA; version 2.0 of the operating software).

Immunoprecipitation of Insulin Receptor. Confluent cell monolayers in 3.5-cm dishes were permeabilized with digitonin and the labeling experiments performed as described above. Cells were then scraped into lysis buffer [20 mM Tris (pH 7.5) containing 137 mM sodium chloride, 1 mM sodium vanadate, 100 mM sodium fluoride, 0.1% SDS, 0.5% sodium deoxycholate, 1% Triton X-100, 0.2% sodium azide, 0.2 mM phenylmethanesulfonyl fluoride, 1 mM benzamidine, 8 μg/mL aprotinin, and 2 μg/mL leupeptin] and the cell lysates incubated for 60 min on ice. After centrifugation (14000*g*, 20 min) to remove cell debris, the supernatant was incubated at 4 °C for 18 h with the monoclonal anti-insulin receptor antibody 29B4 that had been prebound to protein G Plus/protein A–agarose beads; the beads were washed and the antibody–receptor complexes eluted with Laemmli sample buffer containing 5% 2-mercaptoethanol. Proteins were separated on 4–12% gradient (Novex) SDS–PAGE gels under reducing conditions.

Immunoprecipitation of IRS-1. Confluent cell monolayers in 10-cm dishes were permeabilized with digitonin for 20 min at room temperature after which the cell releasate was collected and saved on ice while the cell ghosts, still adherent to the culture dishes, were scraped into lysis buffer. After incubation for 60 min on ice, the cell ghost lysates were centrifuged (100000*g*, 20 min at 4 °C) to sediment cell debris, and the supernatant was incubated for 16 h at 4 °C with a polyclonal anti-human IRS-1 antibody. The cell releasate was incubated with a 2 × concentrated lysis buffer followed by addition of the polyclonal anti-human IRS-1 antibody. The antibody–IRS-1 complexes were immunoprecipitated with protein A–agarose beads; the beads were washed, and the antibody–IRS-1 complexes were eluted with Laemmli sample buffer containing 5% 2-mercaptoethanol. Proteins were separated on 4–12% gradient SDS–PAGE gels under reducing conditions.

Western Blot Analyses. After SDS–PAGE, the proteins were transferred electrophoretically to PVDF membranes in the presence of Rainbow molecular weight markers to assess the quality of the transfer. Membranes were then incubated for 1 h at room temperature in blocking buffer composed of 5% (w/v) non-fat dry milk powder in TBS-T (20 mM Tris, 137 mM sodium chloride, pH 7.6, and 0.1% Tween 20), after which they were incubated overnight at 4 °C with the appropriate primary antibody diluted in the blocking buffer. Membranes were washed 3 times with TBS-T and incubated for 1 h at room temperature with a secondary antibody [either goat anti-mouse or donkey anti-rabbit IgG] coupled to horseradish peroxidase. After three washes, the membranes were developed using the ECL chemoluminescence detection system. Autoradiograms were scanned and quantitated using 1-D AnalystTM software (version 1.1) on a BioRad 620 CCD Densitometer (Richmond, CA). More stringent conditions were needed with the polyclonal antiserum AB-50; 0.1% Tween 20 was replaced with 1% NP-40 in both the blocking and washing buffers. Antiserum AB-50 was raised against an epitope of the carboxy-terminal region of the human insulin receptor.

Tyrosine Kinase Assays. Confluent cell monolayers in 24-multiwell dishes (Costar) were permeabilized with digitonin for 20 min at room temperature in permeabilization medium B that contained, at final concentrations, 35 μg/mL digitonin, 20 mM Tris (pH 7.5), 125 mM potassium chloride, 5 mM sodium chloride, and 11.1 mM glucose. Culture dishes with the cells still in permeabilization medium were transferred to the cooling plate; the insulin receptors were activated by sequential incubation with or without 100 nM insulin (15 min at 6 °C) followed by 20 μM unlabeled ATP with 4 mM manganese chloride (6 °C, 15 min). The medium was removed, and substrate phosphorylation assays were initiated by addition of phosphorylation medium to yield final concentrations of 20 μM [γ-^{32}P]ATP (4–5 μCi/nmol) and 4 mM manganese chloride; peptide 983–993 was used in a range of concentrations. Substrate phosphorylation reactions were terminated after 20–60 min at 6 °C by transferring aliquots of the reaction mixtures into 2 × concentrated Tricine sample buffer (Novex). ^{32}P-Labeled peptide was resolved on 10–20% gradient (Novex) Tricine/SDS–PAGE gels under reducing conditions; these gradient gels separate the phosphorylated peptide from ATP and P_i. After electrophoresis, the gels were dried at 60 °C and exposed to film at −70 °C. ^{32}P-Labeled phosphopeptide was identified by autoradiography and excised from the gel; the incorporated radioactivity was determined by Cerenkov counting. The substrate phosphorylation reaction was linear up to 90 min at 6 °C.

Phosphopeptide and Phosphoamino Acid Analyses. The labeling reactions were performed at 18 °C as described above. After two-dimensional nonreducing/reducing SDS–PAGE electrophoresis (Bernier et al., 1988), the proteins were transferred electrophoretically to PDVF membranes. The radioactive receptor β-subunit was located on the filter membrane by autoradiography and excised. The minced membrane pieces were rehydrated and incubated for 18 h in 50 mM ammonium bicarbonate buffer containing 50 μg/mL L-1-(tosylamino)-2-phenylethyl chloromethyl ketone-treated trypsin (Worthington). Two-dimensional phosphopeptide mapping of the trypic digest was performed on 20 × 20 cm cellulose thin-layer plates by a method similar to that reported earlier (Issad et al., 1991) where 10 μL of the lyophilized and reconstituted reaction mixture was spotted. Electrophoresis in the first dimension was performed at 10 °C for 4 h at 400 V in pH 3.5 electrophoresis buffer containing acetic acid/water/pyridine (10:89:1, v/v), and ascending chromatography in the second dimension was carried out using butanol/acetic acid/water/pyridine (15:3:12:10, v/v) as the mobile phase. ^{32}P-Labeled phosphopeptides were identified by autoradiography. Phosphoamino acid analysis was performed on the receptor β-subunit bound to PDVF membrane as previously reported (Kamps & Sefton, 1989). After hydrolysis with constant-boiling 6 N HCl (Pierce) at 110 °C for 1 h under nitrogen, the liberated phosphoamino acids were separated by electrophoresis at 10 °C in the presence of unlabeled standards on cellulose thin-layer plates for 1.5 h at 1000 V in water/pyridine/acetic acid (189:1:10, v/v), pH 3.5.

RESULTS

Insulin Receptor Phosphorylation in Digitonin-Permeabilized CHO/HIRc Cells. Autophosphorylation of the

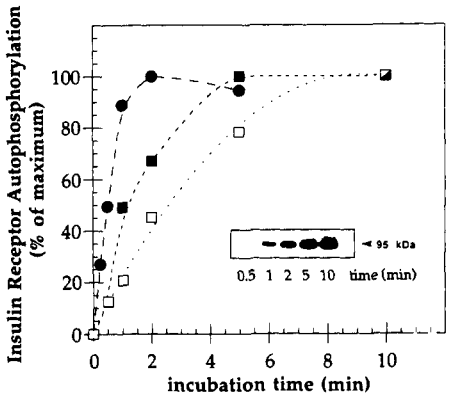

FIGURE 1: Temperature effect on the rate of phosphorylation of insulin receptors in permeabilized cells. Chinese hamster ovary (CHO) cells that had been transfected with the cDNA encoding the normal human insulin receptor (CHO/HIRc) were grown in culture. Cells were incubated in digitonin-containing permeabilization buffer for 20 min at room temperature; the dishes were transferred to a temperature-controlled plate. After 2 min, insulin (100 nM) was added; 15 min later, the phosphorylation reaction was initiated by the addition of 4 mM $MnCl_2$ and 100 μM [γ-^{32}P]ATP (130 μCi/mL) (time = 0). To terminate the experiments, cells were rapidly frozen in liquid nitrogen and lysed; insulin receptors in the membranes were solubilized and recovered by chromatography on wheat germ agglutinin–agarose. The receptors in the eluates were subjected to SDS–PAGE under reducing conditions with quantitative analysis of the dried gels by Betagen counting. ^{32}P labeling of the insulin receptor at each time point was normalized to the maximal level of labeling observed at each temperature: (●) 34 °C; (■) 18 °C; (□) 6 °C. The results represent the average of three to five independent experiments, each of which was performed on duplicate dishes. *Inset*: autoradiograph of the 95-kDa β-subunit from a representative time-course experiment performed at 6 °C.

β-subunit of the insulin receptor was increased 6–8-fold with 100 nM insulin at all three temperatures tested (6, 18, 34 °C) (Figure 1). Both the initial rate of phosphorylation and the time needed to reach maximal levels of receptor labeling were correlated with temperature. These apparent steady-state levels of receptor phosphorylation were maintained for at least 3 min. Significant ATP hydrolysis occurred in the experiments at 34 °C (40% in 2 min) which could account for the decline from the maximal level of receptor labeling after 5 min of incubation (not shown); little or no ATP hydrolysis was observed at 6 or 18 °C.

The labeling of insulin receptors under basal conditions and in the presence of insulin was due exclusively to phosphotyrosine, with no detection of phosphoserine or phosphothreonine (Figure 2). Two-dimensional phosphopeptide maps of trypsin digests of the ^{32}P-labeled β-subunit revealed that ^{32}P incorporation occurred in a number of phosphopeptides (Figure 3) in a pattern of phosphorylation very similar to the pattern of phosphotyrosine-containing peptides observed in freshly isolated liver cells incubated with insulin and [^{32}P]P_i (Issad et al., 1991). There was a predominance of the tris-phosphorylated form of the 1146-kinase[2] domain, with lesser amounts of mono- and bis-phosphorylated forms of the same domain, as well as peptides with two phosphotyrosine residues that are close to the C-terminus of the β-subunit.

Rate of Insulin Receptor Dephosphorylation. To study the dephosphorylation of the insulin receptor, autophosphorylation was stopped by the addition of EDTA (to inactivate kinase activity) and a 40-fold excess of unlabeled ATP (to dilute the concentration of [γ-^{32}P]ATP). The [^{32}P]phos-

[2] The number system used represents that of the minus (–) exon 11 variant receptor.

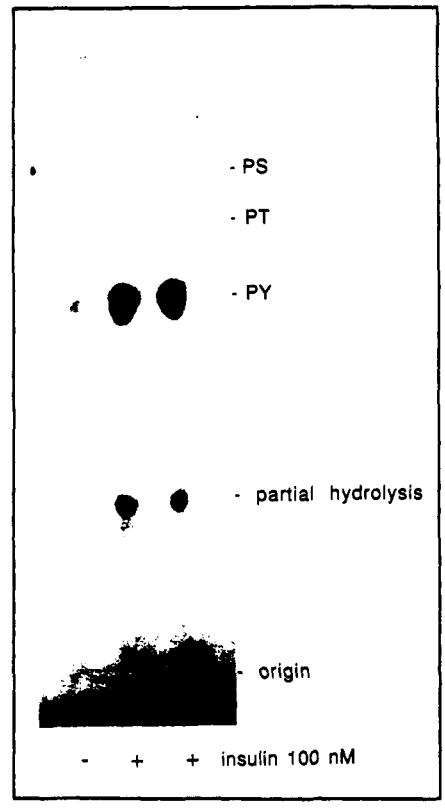

FIGURE 2: Phosphoamino acid analysis of the phosphorylated insulin receptor. Insulin receptors from permeabilized CHO/HIRc cells were autophosphorylated at 18 °C in the absence (lane 1) or the presence of 100 nM insulin (lanes 2 and 3) and processed as described in the legend of Figure 1. Proteins were resolved by two-dimensional nonreducing/reducing SDS–PAGE and electrotransferred to a poly(vinylidene difluoride) (PVDF) membrane. The ^{32}P-labeled receptor β-subunit was localized by autoradiography and excised. After hydrolysis in 6 N HCl, the phosphoamino acids liberated from the receptor β-subunit were analyzed by one-dimensional high-voltage electrophoresis on thin-layer cellulose plates in the presence of unlabeled standards followed by autoradiography. PY, phosphotyrosine; PT, phosphothreonine; PS, phosphoserine. The radioactive spots detected below the amino acid markers are due to incompletely hydrolyzed insulin receptor fragments.

photyrosine content of the receptor β-subunit decreased with a $t_{1/2}$ of ~40 s at 18 °C, and ~120 s at 6 °C (Figure 4).

The rate of dephosphorylation was affected by temperature to about the same extent as the rate of phosphorylation. We did not observe complete dephosphorylation of the receptor at any of the temperatures tested.

Immunoblots probed with an antibody raised against the C-terminus of the human insulin receptor revealed the same amount of β-subunit was present at each dephosphorylation time-point (not shown). This indicates that the loss of label from the receptor β-subunit was not due to losses of receptor itself, and is consistent with the notion that the dephosphorylation of the insulin receptor is mediated by PTPases. The stable fraction of phosphorylated receptor (~30% of total) that remained was resistant to further dephosphorylation. These data are in agreement with those of King et al. (1991). They found that a substantial portion of the [^{32}P]phosphotyrosine at autophosphorylation sites on the insulin receptor persisted after long incubation with PTPases. Finally, dephosphorylation was completely inhibited by vanadate, a known inhibitor of protein tyrosine phosphatases.

Autophosphorylation and Dephosphorylation of a C-Terminally Truncated Insulin Receptor in Permeabilized Cells. We then studied the contribution of the C-terminal domain of the insulin receptor to the observed receptor dephospho-

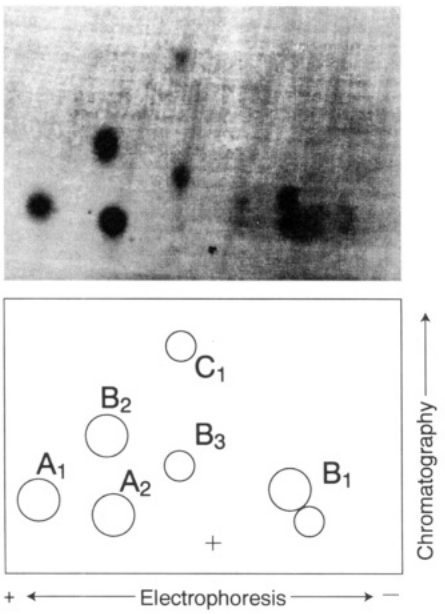

FIGURE 3: Phosphopeptide analysis of the phosphorylated insulin receptor β-subunit. Permeabilized CHO/HIRc cells were incubated in the presence of 100 nM insulin; the insulin receptors were labeled and resolved as described in the Figure 2 legend. The region corresponding to the 95-kDa receptor β-subunit band was excised from the PVDF membrane and incubated with trypsin. The resulting peptides were resolved by two-dimensional phosphopeptide mapping. Top panel: autoradiogram showing the separation of various ^{32}P-labeled phosphopeptides. The bottom panel depicts the locations of phosphotyrosine-containing peptides that had been previously identified from a trypsin digest of the receptor β-subunit phosphorylated in intact liver cells (Issad et al., 1991). Autophosphorylation of tyrosines-1146, -1150, and -1151 in the kinase domain gives rise to a family of five phosphopeptides which are mono (C1), bis (B2 and B3), or tris (A1 and A2) phosphorylated; all are cleaved by trypsin at Arg-1143 and either Arg-1152 (C1, B3, and A2) or Lys-1153 (B2 and A1). Phosphorylated tyrosines-1316 and -1322 are recovered as a bis-phosphorylated peptide that runs as peptide B1. The position of the origin of sample application (+) is shown.

rylation seen in CHO/HIRc cells by using CHO cells transfected with a mutated form of the receptor with a deletion of 43 amino acids at the C-terminus of the β-subunit (CHO/ΔCT cells). We found identical affinities for insulin in both cell lines (3–5 nM), but the CHO/HIRc cells had a binding capacity of 300 fmol/cell vs 220 fmol/cell in CHO/ΔCT cells (Scatchard analysis; data not shown). The latter finding was confirmed by scanning densitometric analysis of the insulin receptor α-subunit immunoblots (result not shown).

The relative rates of insulin-stimulated receptor phosphorylation expressed as a percentage of the maximal incorporation were nearly identical in both cell lines at both 6 and 18 °C (Table 1). The extent of insulin receptor phosphorylation in the presence or absence of insulin was investigated next by comparing the ratio of ^{32}P-phosphorylated receptor β-subunit (by betagen readings of the immunoblotted PVDF membrane) to total receptor content (scanning densitometric analysis of the insulin receptor α-subunit on the same immunoblots) in the two cell lines. We observed a nearly 5-fold increase over basal in insulin-stimulated receptor autophosphorylation in CHO/HIRc cells and a 9-fold increase in CHO/ΔCT cells (Figure 5). The enhanced effect seen in permeabilized CHO/ΔCT cells was due both to a reduction in the basal response and to an increase in the stimulated responses.

The intact insulin receptor contains two tyrosyl residues near the C-terminus of the β-subunit that are autophosphorylated in response to insulin stimulation. These two phosphorylation sites are absent in the truncated receptor. Thus, for the same number of fully phosphorylated receptors, an approximately 30% reduction in the overall [^{32}P]phosphate content in the truncated receptor (compared to the intact receptor) is predicted. When this factor is used to normalize our data, we found a nearly 2-fold greater increase in receptor autophosphorylation in CHO/ΔCT cells after stimulation with insulin when compared to CHO/HIRc cells.

As shown in Figure 6, the rate of loss of [^{32}P]phosphate from insulin receptor in permeabilized CHO/ΔCT cells was comparable to the rate seen in CHO/HIRc cells which suggests that the deleted C-terminal 43 amino acid portion of the insulin receptor is not required to direct efficient dephosphorylation of the receptor. Therefore, it appears that the observed higher steady-state level of insulin receptor autophosphorylation in CHO/ΔCT cells is not due to a reduced rate of receptor dephosphorylation.

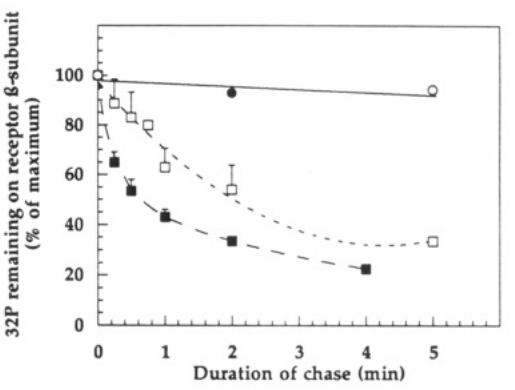

FIGURE 4: Time- and temperature-dependent dephosphorylation of ^{32}P-labeled insulin receptors. Permeabilized CHO/HIRc cells were labeled in the presence of 100 nM insulin at 6 or 18 °C until the maximal level of receptor autophosphorylation was reached, as described in the Figure 1 legend. The autophosphorylation reaction was stopped (time = 0) by incubating the cells at 6 °C (*open symbols*) or 18 °C (*closed symbols*) with a chase solution (unlabeled ATP and EDTA) in the absence (□, ■) or the presence (○, ●) of 200 μM vanadate. The residual phosphorylation was evaluated at the indicated times by transferring the cells to liquid nitrogen; the ^{32}P-labeled insulin receptors were recovered and separated by SDS–PAGE under reducing conditions with quantitative analysis of the dried gels with a Betascope 603 analyzer. The amount of ^{32}P-labeled receptors remaining at each time point was expressed as a percentage of the maximum (no chase reaction) observed at each temperature. The results represent the average ± SEM of three independent experiments, each of which was performed on duplicate dishes.

Table 1: Rate of Insulin Receptor Autophosphorylation at Two Temperatures[a]

incubation time (min)	temp (°C) of incubation: 6 CHO/HIRc	6 CHO/ΔCT	18 CHO/HIRc	18 CHO/ΔCT
0.5	10.85	7		
1	16.3	27.8	51.2	49.9
2	46.2	47.1	70.2	68.4
5	68.3	63.6	100	100
10	100	100		

[a] The rate of autophosphorylation of insulin receptor in CHO/HIRc cells was compared with that of CHO/ΔCT cells. Insulin receptors from permeabilized cells were autophosphorylated in the presence of 100 nM insulin for the indicated times at either 6 °C or 18 °C, and processed as described in the legend of Figure 1. The results represent the average of two independent experiments, each of which was performed on duplicate dishes. The data are presented as the percent of the maximal level of receptor phosphorylation observed at each temperature.

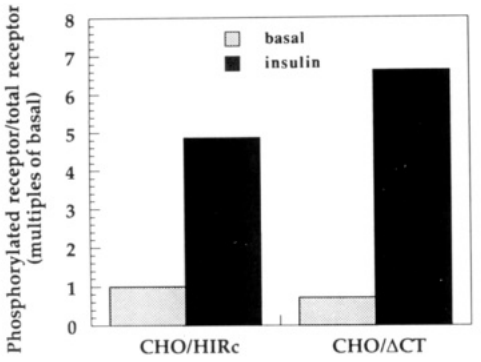

FIGURE 5: Insulin receptor phosphorylation in permeabilized CHO/ΔCT cells. Permeabilized CHO/HIRc cells and CHO/ΔCT cells were incubated in the absence or the presence of 100 nM insulin; insulin receptors were autophosphorylated with [^{32}P]ATP for 5 min at 6 °C, and the cells were lysed in the immunoprecipitation buffer. Insulin receptors present in the lysates were immunoprecipitated with a monoclonal anti-insulin receptor antibody and resolved by SDS–PAGE under reducing conditions, after which the proteins were transferred to PVDF membranes. The results represent the relationship between insulin receptor autophosphorylation and total receptor content. The graph gives the ratio of phosphorylated insulin receptor to total receptors calculated as Betagen readings of the ^{32}P-labeled β-subunit divided by scanning densitometric analysis of the insulin receptor α-subunit immunoblots. The ratio found in the basal state in CHO/HIRc cells has been set to 1, and all the other experimental groups are expressed as multiples of that value.

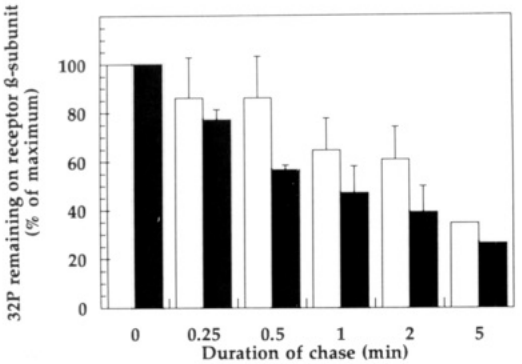

FIGURE 6: Insulin receptor dephosphorylation in permeabilized CHO/ΔCT cells. Permeabilized CHO/HIRc cells (*open bars*) and CHO/ΔCT cells (*closed bars*) were autophosphorylated with [^{32}P]-ATP in the presence of 100 nM insulin for 5 min at 6 °C, and the dephosphorylation reaction was carried out as described in the Figure 4 legend. At each time point, insulin receptors were recovered and subjected to SDS–PAGE under reducing conditions, after which quantitative analysis of the dried gels was performed as in the legend of Figure 1. The amount of ^{32}P-labeled receptor β-subunit remaining with increasing duration of chase was expressed as a percentage of the maximum (no chase reaction) for their respective cell line. The results represent the average ± total range of two independent experiments.

Insulin-Dependent Protein Tyrosine Kinase Activities in Permeabilized Cells. The greater efficacy of the insulin receptor tyrosine kinase in permeabilized CHO/ΔCT cells (compared to CHO/HIRc cells) in autophosphorylating the receptor was also observed with phosphorylation of a synthetic peptide substrate. Synthetic peptides derived from the insulin receptor substrate 1 (IRS-1) molecule have been shown to be excellent substrates of the insulin receptor kinase *in vitro* (Shoelson et al., 1992). We prepared peptide 983–993 (SRGDYMTMQIG) that contains the YMXM motif shown to be a specific recognition domain for several signaling molecules [for a recent review, see Kahn et al. (1993)]. Permeabilized cells were treated with or without insulin, followed by the initiation of receptor autophosphorylation at 6 °C. The medium was removed and replaced with labeling

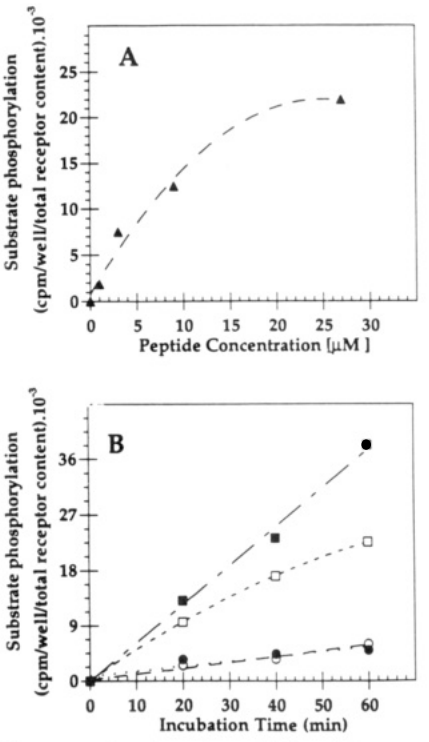

FIGURE 7: Concentration dependence (A) and time course (B) for exogenous substrate phosphorylation in permeabilized cells. CHO/HIRc cells (*open symbols*) and CHO/ΔCT cells (*closed symbols*) were grown to confluence in 24-multiwell dishes. After permeabilization with digitonin, insulin receptors were autophosphorylated in the absence (○, ●) or presence (□, ■, ▲) of 100 nM insulin for 15 min at 6 °C. The medium was removed and replaced with the phosphorylation medium that contained exogenous peptide 983–993 as described under Experimental Procedures. (A) The amount of peptide was varied as shown; phosphorylation assays were for 30 min at 6 °C. (B) Reaction times for phosphorylation of peptide 983–993 (27 μM) were varied as indicated. Results are from a representative of two separate experiments; each data point was obtained from duplicate wells.

medium containing 20 μM [γ-^{32}P]ATP/4 mM Mn^{2+} and a range of concentrations of synthetic peptide as described under Experimental Procedures.

Half-maximal and maximal substrate phosphorylations were observed at peptide concentrations of approximately 7 and 27 μM, respectively (Figure 7A). As shown in Figure 7B, levels of substrate phosphorylation in the absence of insulin were identical in the two cell lines; however, the rate of insulin-stimulated substrate phosphorylation was about 40% higher in the CHO/ΔCT cells, reflecting higher levels of receptor autophosphorylation. A 4-fold activation and a 6-fold activation over basal were obtained following insulin stimulation of permeabilized CHO/HIRc and CHO/ΔCT cells, respectively.

Immunoblot Analysis. Since activation of several insulin signaling pathways involves phosphorylation of the IRS-1 molecule [for a recent review, see Kahn et al. (1993)], we performed experiments measuring its relative abundance in permeabilized cells. In these experiments, CHO/HIRc cells were permeabilized, and the cell releasate was collected and saved, while the cell ghosts were scraped into lysis buffer. The IRS-1 proteins present in both releasate and ghost lysate were immunoprecipitated with an antibody against IRS-1, and the immune pellets were analyzed; IRS-1 was found almost exclusively in the releasate (data not shown). This observed loss in IRS-1 content could possibly alter the pattern of phosphorylation of cellular proteins in response to insulin. To assess this, permeabilized CHO/HIRc cells were exposed to

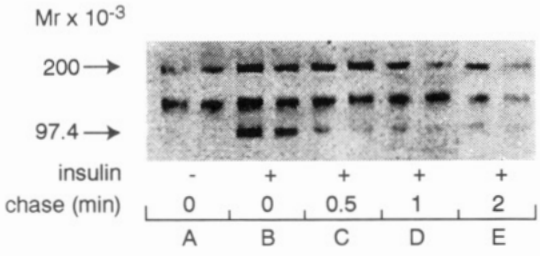

FIGURE 8: Differential dephosphorylation rate of the insulin receptor, pp120, and pp195: phosphotyrosine Western blot analysis. Permeabilized CHO/HIRc cells were phosphorylated with 100 μM unlabeled ATP in the absence (lane A) or the presence (lanes B–E) of 100 nM insulin at 18 °C; cells were either immediately frozen in liquid nitrogen (lanes A and B) (time = 0) or incubated with a chase solution for various times as described in the Figure 4 legend (lanes C–E). The cells were lysed and solubilized, and the clarified lysates were subjected to chromatography on wheat germ agglutinin–agarose. The bound glycoproteins were eluted from the resin, subjected to SDS–PAGE under reducing conditions, electrotransferred to a PVDF membrane, and immunoblotted with anti-phosphotyrosine antibodies. The relative molecular mass standards are shown $\times 10^{-3}$.

insulin, and autophosphorylation of the insulin receptor was initiated by addition of 100 μM unlabeled ATP at 18 °C. The dephosphorylation reaction was then carried out by the addition of the chase solution as outlined under Experimental Procedures. Membrane proteins were solubilized and subjected to chromatography on WGA–Sepharose. The bound glycoproteins, after elution from the resin, were evaluated for their phosphotyrosine content by Western blot analysis with anti-phosphotyrosine antibodies. Three cellular proteins were tyrosine-phosphorylated under the conditions we employed (Figure 8). In addition to the 95-kDa receptor β-subunit, there were two bands: one corresponding to 120 kDa, presumed to be an endogenous tyrosine kinase associated with focal adhesion placques (Schaller et al., 1992); and the other band corresponding to a novel 195-kDa protein. Insulin appeared to stimulate modestly tyrosine phosphorylation of the 195-kDa protein. The phosphotyrosine content of the receptor β-subunit decreased rapidly (Figure 8, lanes B–E), whereas the dephosphorylation of pp195 was considerably slower with a $t_{1/2}$ of $\sim$60 s. Measurable dephosphorylation of pp120 was not evident until the 120-s chase sample.

The pp195 copurified with the insulin receptor on WGA–Sepharose chromatography. It is not related immunologically to the insulin receptor, since pp195 could not be detected in the immune pellets after immunoprecipitation of an aliquot of permeabilized cell lysates with an antibody against human insulin receptor (not shown). Also, the absence of detectable IRS-1 in cell ghosts after permeabilization provides evidence against IRS-1 being pp195. Finally, pp195 was not detected in response to EGF (not shown), ruling out the possibility that pp195 was the EGF receptor.

DISCUSSION

A permeabilization protocol was used to allow careful examination of the rate of phosphorylation and dephosphorylation of insulin receptors using pulse–chase techniques. This approach has been used successfully with rat adipocytes to study the phosphorylation and dephosphorylation of the insulin receptor and an endogenous substrate (Mooney & Anderson, 1989; Mooney & Bordwell, 1992). In the present study, we have shown that the permeabilized CHO cell overexpressing the human insulin receptor is a useful model for examining insulin receptor-related phosphorylation and dephosphorylation as both intact and C-terminal truncated insulin receptors are rapidly autophosphorylated and act as substrates for putative cellular PTPase(s). Two additional cellular proteins were tyrosine-phosphorylated under the conditions we employed (M_r 120 000 and 195 000). In addition, the insulin receptor in this cell model system is able to efficiently phosphorylate an exogenous synthetic substrate related to IRS-1. This latter finding should allow us to use this system to study factors that regulate the dynamics of insulin receptor phosphorylation and dephosphorylation. Such studies may eventually lead to the development of pharmaceutical agents that augment the effects of insulin in insulin-resistant states.

In digitonin-permeabilized CHO/HIRc cells, insulin treatment increased the phosphorylation level of insulin receptor at a rate dependent on the temperature of incubation. As anticipated, a delayed steady-state accumulation of autophosphorylated receptors is produced by a reduction in temperature. Phosphoamino acid analysis indicated only phosphotyrosines in the 95-kDa β-subunit of the receptor, whether phosphorylations were conducted in the absence or presence of insulin. This contrasts with phosphorylation of the receptor in intact cells where a significant level of serine and threonine phosphorylation also occurs (Pang et al., 1985), catalyzed by insulin-stimulated insulin receptor serine kinase(s) (Zick et al., 1983; Smith et al., 1988; Lewis et al., 1990). The absence of phosphoserine suggests the loss of such serine kinase(s) from the permeabilized cells.

The major site of insulin-stimulated phosphorylation was the tris-phosphorylated form of the catalytic region of the insulin receptor. This pattern of phosphorylation is similar to that reported for the intact rat liver (Issad et al., 1991) and intact CHO cells overexpressing human insulin receptors (Tavare et al., 1988; Feener et al., 1993), but contrasts with other findings where only 15–20% of the 1146-kinase domain was found to be tris-phosphorylated (Tornqvist et al., 1988; White et al., 1988b).

Under selected *in vitro* conditions in the presence of high concentrations of ADP and divalent cations, the insulin receptor can be dephosphorylated slowly (over hours) by transfer of phosphate to ADP (Pike et al., 1986; Argetsinger & Shafer, 1992). It is unlikely that these conditions are obtained *in vivo* or in our experiments. The high concentration of the chelator EDTA during the chase reaction rules out the possibility that the insulin receptor kinase itself was involved in the dephosphorylation reaction. The dephosphorylation reaction was independent of the presence of divalent cations, including Ca^{2+}, and was completely inhibited by the PTPase inhibitor vanadate. We therefore conclude that the dephosphorylation of the receptor in our permeabilized cells was mediated by PTPase(s).

Dephosphorylation of the insulin receptor occurred at a temperature (6 °C) that impairs membrane fluidity and markedly slows translational movement of proteins in the membrane. The present study supports the notion that a close association exists between insulin receptor and the protein(s) involved in the dephosphorylation cascade at the cell membrane. Both the rate of phosphorylation and the rate of dephosphorylation of the receptor were affected by temperature to about the same extent. If a physical association between the receptor and a "distant" phosphotyrosine phosphatase is needed to initiate dephosphorylation, one might expect a disproportionate decrease in the dephosphorylation rate at lower temperatures. However, the rapid phosphate turnover we observed in permeabilized cells at 6 °C suggests a constitutive association between insulin receptor and the

protein(s) involved in the dephosphorylation, to form a macromolecular complex which remains intact following the permeabilization procedure.

In permeabilized cells, human insulin receptor containing a deletion of the 43 amino acid C-terminal segment of the β-subunit (and therefore lacking Tyr^{1318} and Tyr^{1322} autophosphorylation sites) was more efficiently autophosphorylated than intact receptor; steady-state levels were approximately twice that of the intact receptor. This finding suggested that under identical conditions the truncated receptor's intrinsic tyrosine kinase activity may be more fully activated than that of the intact receptor. To test this hypothesis, we compared the ability of the two receptor preparations to phosphorylate a synthetic fragment of IRS-1. Both were able to efficiently phosphorylate the synthetic substrate ($K_m \sim 7$ μM). The rate of insulin-stimulated substrate phosphorylation by the truncated receptor was nearly 50% more than that of the intact receptor, confirming the predictive value of the comparative autophosphorylation data. Some investigators have shown that both the truncated and intact insulin receptors have very similar abilities to autophosphorylate and stimulate substrate phosphorylation (Myers et al., 1991; Takata et al., 1991). The reason for these apparent discrepencies is unclear, but may reflect difference(s) in the experimental procedures.

The rate of dephosphorylation of the C-terminal truncated receptor was comparable to that of the intact receptor even though two major phosphorylation sites (Tyr^{1318} and Tyr^{1322}) were missing. This may, at least in part, reflect the fact that the C-terminal domain species of the intact insulin receptor is thought to be dephosphorylated at a significantly slower rate than the tris-phosphorylated 1146-kinase domain (King et al., 1991; Tappia et al., 1991). It is important to note that tris-phosphorylation of the 1146-kinase domain is required for full kinase activation and maximal biological responses (White et al., 1988b; Wilden et al., 1992). Dephosphorylation of this domain correlated with receptor inactivation (King & Sale, 1990; King et al., 1991). Since substantial amounts of the ^{32}P associated with the truncated receptor are likely to be present in this domain, the dephosphorylation rates that we observed in CHO/ΔCT cells should reflect the true rate of receptor deactivation. These findings demonstrate that deletion of the C-terminal 43 amino acid domain of the insulin receptor has little effect on the dephosphorylation pathway, suggesting that this domain of the receptor is not likely to function as a docking site for a PTPase, as recently proposed (Maegawa et al., 1993). However, our results support the possibility that this segment of the receptor may play a role in the regulation of several insulin receptor functions (Maegawa et al., 1988; Ando et al., 1992; Begum et al., 1993).

Permeabilization resulted in the loss of most, if not all, of IRS-1 protein from our cell preparations. Nonetheless, the insulin receptors were autophosphorylated to high steady-state levels, and the receptors were able to efficiently phosphorylate a synthetic substrate. Therefore, it appears that IRS-1 is not necessary for the membrane-bound insulin receptor to perform these functions. Furthermore, it is clear that the rapid kinetics of receptor dephosphorylation observed in these permeabilized cells were obtained in the absence of IRS-1, ruling out the possibilities that IRS-1 could have serve as a docking site for proteins necessary for the dephosphorylation cascade. Although it has not been implicated in the induction of insulin receptor autophosphorylation and tyrosine kinase activity, one could envision the possibility that IRS-1 is important in preventing insulin receptor dephosphorylation. If IRS-1 was indeed involved in hindering the association between insulin receptor and cellular PTPase(s), any manipulation aimed at altering the formation of IRS-1·insulin receptor β-subunit complex should lead to a sharp reduction in the extent of receptor phosphorylation, as PTPases would have a better access to the multiple autophosphorylation sites on the receptor. Thus, the release of most of IRS-1 from permeabilized cells might therefore greatly enhance the rate of insulin receptor dephosphorylation. However, this possibility appears unlikely based on a series of observations made with CHO cells expressing insulin receptors in which a discrete region of the juxtamembrane region has been mutated (either by point mutations or by deletion). In these cell lines, there was a lack of IRS-1 phosphorylation, and yet the balance between phosphorylation and dephosphorylation of the mutated receptors was not affected (White et al., 1988a; Backer et al., 1992). This suggests that the association, or lack of it, between IRS-1 and insulin receptor is not likely to modulate the extent of insulin receptor dephosphorylation.

We have shown the tyrosine phosphorylation of a novel 195-kDa protein in permeabilized CHO/HIRc cells. pp195 is not immunoprecipitated by anti-receptor antibodies, nor does it appear to form a stable complex with the receptor. The retention of pp195 in permeabilized cells suggests its association with the membrane. It adsorbs to a lectin affinity column, suggesting that it is a glycoprotein (although it is possible that it bound to a glycoprotein retained on the column). A tyrosine-phosphorylated glycoprotein of similar size has been detected previously in lectin-purified insulin receptor preparations from rat liver and muscle (Komori et al., 1989), identified recently as negative acute-phase protein 1-inhibitor III (Komori et al., 1992). 1-Inhibitor III has been cloned from various sources including rat liver (Aiello et al., 1988; Braciak et al., 1988) and human hepatoma cells (Koch et al., 1992). Although insulin was unable to promote a strong and consistent enhancement in the phosphorylation of the 195-kDa protein, we cannot rule out the possibility that pp195 subserves an IRS-1-like role. We are currently investigating this possibility.

ACKNOWLEDGMENT

We thank Lisa G. Adams for her expert technical assistance and Paul Ciesla from Photo and Art Unit, NIA. We also thank Dr. S. Mitchell Harman for critical reading of the manuscript.

REFERENCES

Aiello, L. P., Shia, M. A., Robinson, G. S., Pilch, P. F., & Farmer, S. R. (1988), *J. Biol. Chem. 263*, 4013–4022.

Ando, A., Momomura, K., Tobe, K., Yamamoto-Honda, R., Sakura, H., Tamori, Y., Kaburagi, Y., Koshio, O., Akanuma, Y., Yazaki, Y., Kasuga, M., & Kadowaki, T. (1992) *J. Biol. Chem. 267*, 12788–12796.

Argetsinger, L. S., & Shafer, J. A. (1992) *J. Biol. Chem. 267*, 22095–22101.

Backer, J. M., Schroeder, G. G., Kahn, C. R., Myers, M. G., Wilden, P. A., Cahill, D. A., & White, M. F. (1992) *J. Biol. Chem. 267*, 1367–1374.

Begum, N., Olefsky, J. M., & Draznin, B. (1993) *J. Biol. Chem. 268*, 7917–7922.

Bernier, M., Laird, D. M., & Lane, M. D. (1988) *J. Biol. Chem. 263*, 13626–13634.

Boylan, J. M., Brautigan, D. L., Madden, J., Raven, T., Ellis, L., & Gruppuso, P. A. (1992) *J. Clin. Invest. 90*, 174–179.

Braciak, T. A., Northemann, W., Hudson, G. O., Shiels, B. E., Gehring, M. R., & Fey, G. H. (1988) *J. Biol. Chem. 263*, 3999–4012.

Chou, C. K., Dull, T. J., Russell, D. S., Gherzi, R., Lebwohl, D., Ullrich, A., & Rosen, O. M. (1987) *J. Biol. Chem. 262*, 1842–1847.

Debant, A., Clausner, E., Ponzio, G., Filloure, C., Auzan, C., Contreres, J. O., & Rossi, B. (1988) *Proc. Natl. Acad. Sci. U.S.A. 85*, 8032–8036.

Ebina, Y., Araki, E., Taira, M., Shimada, F., Mori, M., Craik, C. S., Siddle, K., Pierce, S. B., Roth, R. A., & Rutter, W. J. (1987) *Proc. Natl. Acad. Sci. U.S.A. 84*, 704–708.

Ellis, L., Clauser, E., Morgan, D. O., Edery, M., Roth, R. A., & Rutter, W. J. (1986) *Cell 45*, 721–732.

Endemann, G., Yonezawa, K., & Roth, R. A. (1990) *J. Biol. Chem. 265*, 396–400.

Faure, R., Baquiran, G., Bergeron, J. J., & Posner, B. I. (1992) *J. Biol. Chem. 267*, 11215–11221.

Feener, E. P., Backer, J. M., King, G. L., Wilden, P. A., Sun, X. J., Kahn, C. R., & White, M. F. (1993) *J. Biol. Chem. 268*, 11256–11264.

Guan, K. L., & Dixon, J. E. (1991) *J. Biol. Chem. 266*, 17026–17030.

Häring, H. V., Kasuga, M., White, M. F., Crettaz, M., & Kahn, C. R. (1984) *Biochemistry 23*, 3298–3306.

Hashimoto, N., Zhang, W. R., & Goldstein, B. J. (1992) *Biochem. J. 284*, 569–576.

Issad, T., Tavare, J. M., & Denton, R. M. (1991) *Biochem. J. 275*, 15–21.

Kahn, C. R., White, M. F., Shoelson, S. E., Backer, J. M., Araki, E., Cheatham, B., Csermely, P., Folli, F., Goldstein, B. J., Huertas, P., Rothenberg, P. L., Saad, M. J. A., Siddle, K., Sun, X. J., Wilden, P. A., Yamada, K., & Kahn, S. A. (1993) *Recent Prog. Horm. Res. 48*, 291–339.

Kamps, M. P. (1989) *Anal. Biochem. 176*, 22–27.

King, M. J., & Sale, G. J. (1988) *Biochem. J. 256*, 893–902.

King, M. J., & Sale, G. J. (1990) *Biochem. J. 266*, 251–259.

King, M. J., Sharma, R. P., & Sale, G. J. (1991) *Biochem. J. 275*, 413–418.

Koch, K. S., Lu, X. P., Brenner, D. A., & Leffert, H. L. (1992) *Biochem. Biophys. Res. Commun. 183*, 184–192.

Komori, K., Block, N. E., Robinson, K. A., & Buse, M. G. (1989) *Endocrinology 125*, 1438–1450.

Komori, K., Robinson, K. A., Block, N. E., Roberts, R. C., & Buse, M. G. (1992) *Endocrinology 131*, 1288–1296.

Laemmli, U. K. (1970) *Nature (London) 227*, 680–685.

Lau, K. H. W., Farley, J. R., & Baylink, D. J. (1989) *Biochem. J. 257*, 23–36.

Lewis, R. E., Wu, G. P., MacDonald, R., & Czech, M. P. (1990) *J. Biol. Chem. 265*, 947–955.

Maegawa, H., McClain, D. A., Freidenberg, G., Olefsky, J. M., Napier, M., Lipari, T., Dull, T. J., Lee, J., & Ullrich, A. (1988) *J. Biol. Chem. 263*, 8912–8917.

Maegawa, H., Ugi, S., Ishibashi, O., Tachikawa-Ide, R., Takahara, N., Tanaka, Y., Takagi, Y., Kikkawa, R., Shigeta, Y., & Kashiwagi, A. (1993) *Biochem. Biophys. Res. Commun. 194*, 208–214.

McClain, D. A., Maegawa, H., Lee, J., Dull, T. J., Ulrich, A., & Olefsky, J. M. (1987) *J. Biol. Chem. 262*, 14663–14671.

Meyerovitch, J., Backer, J. M., & Kahn, C. R. (1989) *J. Clin. Invest. 84*, 976–983.

Mooney, R. A., & Anderson, D. L. (1989) *J. Biol. Chem. 264*, 6850–6857.

Mooney, R. A., & Bordwell, K. L. (1992) *J. Biol. Chem. 267*, 14054–14060.

Myers, M., Backer, J. M., Siddle, K., & White, M. F. (1991) *J. Biol. Chem. 266*, 10616–10623.

Pang, D. T., Sharma, B. R., Shafer, J. A., White, M. F., & Kahn, C. R. (1985) *J. Biol. Chem. 260*, 7131–7136.

Pike, L. J., Eakes, A. T., & Krebs, E. G. (1986) *J. Biol. Chem. 261*, 3782–3789.

Ramachandran, C., Aebersold, R., Tonks, N. K., & Pot, D. A. (1992) *Biochemistry 31*, 4232–4238.

Roome, J., O'Hare, T., Pilch, P. F., & Brautigan, D. L. (1988) *Biochem. J. 256*, 493–500.

Rosen, O. M. (1987) *Science 237*, 1452–1458.

Rosen, O. M., Herrera, R. H., Olowe, Y., Petruzelli, L. M., & Cobb, M. H. (1983) *Proc. Natl. Acad. Sci. U.S.A. 80*, 3237–3240.

Ruderman, N. B., Kapeller, R., White, M. F., & Cantley, L. C. (1990) *Proc. Natl. Acad. Sci. U.S.A. 87*, 1411–1415.

Schaller, M. D., Borgman, C. A., Cobb, B. S., Vines, R. R., Reynolds, A. B., & Parsons, J. T. (1992) *Proc. Natl. Acad. Sci. U.S.A 89*, 5192–5196.

Shoelson, S. E., Chatterjee, S., Chaudhuri, M., & White, M. F. (1992) *Proc. Natl. Acad. Sci. U.S.A. 89*, 2027–2031.

Smith, D. M., King, M. J., & Sale, G. J. (1988) *Biochem. J. 250*, 509–519.

Streuli, M., Krueger, N. X., Thai, T., Tang, M., & Sato, H. (1990) *EMBO J. 9*, 2399–2407.

Takata, Y., Webster, N. J. G., & Olefsky, J. M. (1991) *J. Biol. Chem. 266*, 9135–9139.

Tappia, P. S., Sharma, R. P., & Sale, G. J. (1991) *Biochem. J. 278*, 69–74.

Tavare, J. M., O'Brien, R. M., Siddle, K., & Denton, R. M. (1988) *Biochem. J. 253*, 783–788.

Tonks, N. K., Charbonneau, H., Diltz, C. D., Kumar, S., Cicirelli, M. F., Krebs, E. G., Walsh, K. A., & Fisher, E. H. (1989) *Adv. Protein Phosphatases 5*, 149–180.

Tornqvist, H. E., Gunsalus, J. R., Nemenoff, R. A., Frackelton, A. R., Pierce, M. W., & Avruch, J. (1988) *J. Biol. Chem. 263*, 350–359.

White, M. F., Stegmann, E. W., Dull, T. J., Ullrich, A., & Kahn, C. R. (1987) *J. Biol. Chem. 262*, 9769–9777.

White, M. F., Livingston, J. N., Backer, J. M., Lauris, V., Dull, T. J., Ullrich, A., & Kahn, C. R. (1988a) *Cell 54*, 641–649.

White, M. F., Shoelson, S. E., Keutmann, H., & Kahn, C. R. (1988b) *J. Biol. Chem. 263*, 2969–2980.

Wilden, P., Siddle, K., Haring, E., Backer, J. M., White, M. F., & Kahn, C. R. (1992) *J. Biol. Chem. 267*, 13719–13727.

Zick, Y., Kasuga, M., Kahn, C. R., & Roth, J. (1983) *J. Biol. Chem. 258*, 75–80.